J|A|C|S
A R T I C L E S

UltraSOFAST HMQC NMR and the Repetitive Acquisition of 2D Protein Spectra at Hz Rates

Maayan Gal,[†] Paul Schanda,[‡] Bernhard Brutscher,[‡] and Lucio Frydman*,[†]

Contribution from the Department of Chemical Physics, Weizmann Institute of Science, 76100 Rehovot, Israel, and Institut de Biologie Structurale, Jean-Pierre Ebel C.N.R.S.-C.E.A.-UJF, 41, rue Jules Horowitz, 38027 Grenoble Cedex 1, France

Received October 3, 2006; E-mail: lucio.frydman@weizmann.ac.il

Abstract: Following unidirectional biophysical events such as the folding of proteins or the equilibration of binding interactions, requires experimental methods that yield information at both atomic-level resolution and at high repetition rates. Toward this end a number of different approaches enabling the rapid acquisition of 2D NMR spectra have been recently introduced, including spatially encoded "ultrafast" 2D NMR spectroscopy and SOFAST HMQC NMR. Whereas the former accelerates acquisitions by reducing the number of scans that are necessary for completing arbitrary 2D NMR experiments, the latter operates by reducing the delay between consecutive scans while preserving sensitivity. Given the complementarities between these two approaches it seems natural to combine them into a single tool, enabling the acquisition of full 2D protein NMR spectra at high repetition rates. We demonstrate here this capability with the introduction of "ultraSOFAST" HMQC NMR, a spatially encoded and relaxation-optimized approach that can provide 2D protein correlation spectra at ~1 s repetition rates for samples in the ~2 mM concentration range. The principles, relative advantages, and current limitations of this new approach are discussed, and its application is exemplified with a study of the fast hydrogen−deuterium exchange characterizing amide sites in Ubiquitin.

1. Introduction

Multidimensional nuclear magnetic resonance (NMR) spectroscopy is a widely used tool in the study of biomolecular dynamics. Fluctuations in proteins and nucleic acids on a pico- to millisecond time scale are best studied by relaxation measurements, residual dipolar couplings, or spectral line shapes;[1−3] unidirectional dynamic changes such as the exchange of amide protons for deuterons (H/D exchange) or the progression of an unfolded ensemble toward a folded structure can be more naturally followed by real-time NMR spectral changes.[4−6] An important limitation to such real-time measurements comes from the fact that conventional 1D NMR spectroscopy lacks the resolution needed to cope with multiple overlapping lines; on the other hand, the 2D NMR methods that are capable of resolving the individual atomic peaks arising from a macromolecule are intrinsically time-consuming. These longer acquisition times come as a result of the manner by which the data, and in particular the indirect-domain spectral components, are sampled in 2D NMR.[7,8] Whereas the t_2 domain is directly

monitored in 2D acquisitions by physical digitization, the indirect-domain evolution is recorded by repeating the pulse sequence numerous times in association with increments of a corresponding delay parameter t_1. Given the identical Nyquist criteria defining bandwidth and resolution along both time domains this means that, even if sensitivity is sufficient to monitor the data being sought in a single scan, multiple repetitions will still have to be performed. The total experimental time will in such cases be given by the number of scans N_{scans} required for appropriately sampling the indirect domain, multiplied by a single-scan duration T_{scan} usually dominated by the need for allowing spins to relax back to thermal equilibrium prior to repeating an additional measurement. In contemporary protein NMR spectroscopy this recycle delay is associated with a ^{1}H spin-lattice relaxation time T_1 on the order of seconds; this in turn translates into acquisition times on the order of minutes even for the most sensitive kinds of 2D NMR experiments. Very rapid repetition rates on the order of Hz, which might be of great interest for the study of fast biomolecular events, are therefore unavailable to standard real-time 2D NMR acquisitions.

Driven partly by this need recent years have witnessed an increased interest in accelerating the acquisition of 2D NMR data, and to this end several methods have been proposed.[9] In general terms these methods can be catalogued as acting either by reducing the T_{scan} repetition delay between the various increments or by decreasing the overall number N_{scans} of scans

[†] Weizmann Institute of Science.
[‡] Institut de Biologie Structurale−Jean-Pierre Ebel C.N.R.S.-C.E.A.-UJF.
(1) Palmer A. G., III. *Chem. Rev.* **2004,** *104,* 3623−3640.
(2) Blackledge, M. *Prog. Nucl. Magn. Reson. Spectrosc.* **2005***, 46,* 23−61.
(3) Mittermayer, A. M.; Kay, L. E. *Science* **2006**, *312,* 224−228.
(4) Dobson, C. M.; Hore, P. J. *Nat. Struc. Biol.* **1998**, *5,* 504−507.
(5) Dempsey, C. E. *Prog. Nucl. Magn. Reson. Spectrosc.* **2001**, *39,* 135−170.
(6) Zeeb, M.; Balbach, J. *Methods Enzymol.* **2004**. *34,* 65−74.
(7) Jeener, J. Oral presentation in Ampere International Summer School II, Basko Polje, Yugoslavia, 1971.
(8) Aue, W. P.; Bartholdi, E.; Ernst, R. R. *J. Chem. Phys.* **1976,** *64,* 2229−2240.
(9) Freeman, R.; Kupce, E. *J. Biomol. NMR* **2003**, *27,* 101−113.

needed to retrieve the spectra. The former group aims at maximizing sensitivity while allowing for very short recycle delays; this can be achieved by accelerating the spin-lattice relaxation of the spins of interest,[10,11] and in certain specific experiments by relying on optimized flip-angles (e.g., the Ernst angle[12]) to enhance the steady-state magnetization of the excited spins.[13] Moreover, proposals have been recently made that combine these two features into single 2D and 3D NMR protocols,[14–16] including the band-selective optimized flip-angle short-transient HMQC (SOFAST HMQC) NMR experiment. SOFAST HMQC enables a reduction of T_{scan} down to ≤ 100 ms while preserving high sensitivity, thus allowing for the recording of conventionally sampled 2D ^{1}H-^{15}N or ^{1}H-^{13}C correlation spectra within minimal experimental times of just several seconds. Important among the group of experiments whose aim is to reduce the total number of necessary N_{scans} count accordion and projection NMR methods,[17–21] Hadamard spectroscopy,[22,23] and other ingenious schemes that carry a nonlinear sampling of data points together with an appropriate data processing.[24–27] Arguably, the most dramatic reduction in the number of required scans is achieved by "ultrafast" NMR; a protocol which allows one to record arbitrarily high multidimensional NMR data sets within a single transient.[28–30] At the heart of this approach lies replacing the stepwise incrementation of the temporal parameter t_1 involved in 2D NMR, by an analogous encoding of the indirect-domain evolution along a spatial dimension z. This procedure can be carried out in a variety of different ways, usually involving the combined application of pulsed field gradients and frequency-swept spin manipulations that replace the $\Omega_1 t_1$ time encoding by an analogous $C\Omega_1(z - z_o)$ spatial encoding—with $C \approx t_1^{max}/$(sample length) a constant under our control and z_o denoting an arbitrary spatial origin. The spatial winding of the spins entailed by this phase expression is preserved, just as in traditional 2D NMR experiments, by a coherent mixing scheme, to be subsequently unwound and read out over the course of the data acquisition using pulsed field gradients. This reading process can be repeated numerous times by oscillating the sign of the readout field gradients, allowing one to monitor a set of indirect-domain spectra as a function of the direct-domain t_2 evolution. Fourier

transformation of the resulting data along t_2 thus provides the full $I(\Omega_1,\Omega_2)$ spectral information being sought, within a single transient.

Although the spatially encoded NMR principles just described can yield 2D NMR spectra within a single scan, a full dynamic characterization will in general entail collecting a large number of transients. This demand will be intrinsic to real-time methods that look at unidirectional biomolecular processes by monitoring the full range of 2D NMR spectral changes occurring as a function of time. Moreover, even if ultrafast NMR makes the acquisition of 2D data feasible within a single scan, practical sensitivity and solvent suppression considerations often demand the signal averaging of at least a minimal number of transients. Indeed, contemporary NMR hardware limits the per-scan sensitivity of ultrafast 2D acquisitions to the low-mM range;[31] these concentrations may exceed those typically encountered in biomolecular measurements attempting to detect transient chemical species, implying that several scans may have to be averaged anyhow to achieve an acceptable signal-to-noise ratio (SNR). Bearing these needs in mind, it becomes clear that, even when considering the use of single-scan 2D NMR within a real-time biomolecular dynamic setting, this approach could also benefit from protocols that shorten the repetition delay T_{scan} while preserving maximum SNR. The present study explores such possibility by demonstrating that, if the very short interscan delays afforded by the SOFAST protocol are merged with the single-scan capabilities of ultrafast NMR, full 2D protein correlation spectra can be repeatedly retrieved at unprecedented rates. A number of provisions to be taken into account for maximizing the efficiency of the resulting "ultraSOFAST" NMR experiment are discussed, its ability to acquire real-time 2D NMR spectra of proteins undergoing a unidirectional dynamic process at mM concentrations within 1–2 s experimental times is illustrated, and its benefits and drawbacks vis-à-vis other recent proposals are compared.

2. Methods

Different variants could be considered for combining the single-scan capabilities of ultrafast NMR with the rapid repetition benefits of SOFAST protocols. The pulse sequence chosen to test the general performance of such spatially encoded 2D variants is shown in Figure 1A; shown also for completeness in the Figure is an additional amplitude-modulated (am) ultrafast HSQC sequence previously proposed to obtain ^{1}H-^{15}N 2D protein correlations in real-time.[32] As the new sequence in Figure 1A incorporates a SOFAST excitation it also possesses the main features of this experiment.[14,15] First, it applies all ^{1}H pulses band-selectively on the subset of protons that are of interest— in this case the amide protons—while leaving all other protons unperturbed. This assists in efficiently relaxing the excited spins, significantly decreasing their effective spin-lattice relaxation time T_1. Second, instead of relying on a $\pi/2$ ^{1}H excitation, a partial excitation optimized for short recycle delays (with flip angles $\alpha \approx 120°$ followed by a 180° refocusing for $T_{scan} \approx 100$–300 ms) is employed to further enhance sensitivity per unit acquisition time. The new pulse sequence also incorporates spatial encoding to monitor the indirect-domain ^{15}N-dimension using a constant-time evolution period based on bipolar gradients and linear radiofrequency π sweeps scanning the sample in identical frequency directions.[37] This was preferred over alternative

(10) Pervushin, K.; Voegeli, B.; Eletsky, A. *J. Am. Chem. Soc.* **2002**, *124*, 12898−12902.
(11) Diercks, T.; Daniels, M.; Kaptein, R. *J. Biomol. NMR* **2005**, *33*, 243−259.
(12) Freeman, R.; Hill, H. D. W. *J. Magn. Reson.* **1971**, *4*, 366−383.
(13) Ross, A.; Salzmann, M.; Senn, H. *J. Biomol. NMR* **1997**, *10*, 289−296.
(14) Schanda, P.; Brutscher, B. *J. Am. Chem. Soc.* **2005**, *127*, 8014−8015.
(15) Schanda, P.; Kupce, E.; Brutscher, B. *J. Biomol. NMR* **2005**, *33*, 199−211.
(16) Schanda, P.; Van Melckebeke, H.; Brutscher, B. *J. Am. Chem. Soc.* **2006**, *128*, 9042−9043.
(17) Szyperski, T.; Wider, G.; Bushweller, J. H.; Wuthrich, K. *J. Am. Chem. Soc.* **1993**, *125*, 9307−9308.
(18) Ding, K.; Gronenborn, A. *J. Magn. Reson.* **2002**, *156*, 262−268.
(19) Bersch, B.; Rossy, E.; Coves, J.; Brutscher, B. *J. Biomol. NMR* **2003**, *27*, 57−67.
(20) Kim, S.; Szyperski, T. *J. Am. Chem. Soc.* **2003**, *125*, 1385−1393.
(21) Kupce, E.; Freeman, R. *J. Am. Chem. Soc.* **2003**, *126*, 6429−6440.
(22) Kupce, E.; Nishida, T.; Freeman, R. *Prog. Nucl. Magn. Reson. Spectrosc.* **2003**, *42*, 95−122.
(23) Brutscher, B. *J. Biomol. NMR* **2004**, *29*, 57−64.
(24) Mandelshtam, V. A. *J. Magn. Reson.* **2000**, *144*, 343−356.
(25) Hoch, J. C.; Stern, A. S. *NMR Biol. Macromol.* **2001**, *Part A*, 159−178.
(26) Rovnyak, D.; Frueh, D. P.; Sastry, M.; Sun, Z. Y. J.; Stern, A. S.; Hoch, J. C.; Wagner, G. *J. Magn. Reson.* **2004**, *170*, 15−21.
(27) Brüschweiler, R.; Zhang, F. *J. Chem. Phys.* **2004**, *120*, 5253−5260.
(28) Frydman, L.; Scherf, T.; Lupulescu, A. *Proc. Natl. Acad. Sci. U.S.A.* **2002**, *99*, 15858−15862.
(29) Frydman, L.; Lupulescu, A.; Scherf, T. *J. Am. Chem. Soc.* **2003**, *125*, 9204−9217.
(30) Shrot, Y.; Frydman, L. *J. Am. Chem. Soc.* **2003,** *125,* 11385−11396.

(31) Shapira, B.; Lupulescu, A.; Shrot, Y.; Frydman, L. *J. Magn. Reson.* **2004**, *166*, 152−163.
(32) Gal, M.; Mishkovsky, M.; Frydman, L. *J. Am. Chem. Soc.* **2006**, *128*, 951−956.
(33) Kupce, E.; Freeman, R. *J. Magn. Reson. A* **1994**, *108*, 268−273.
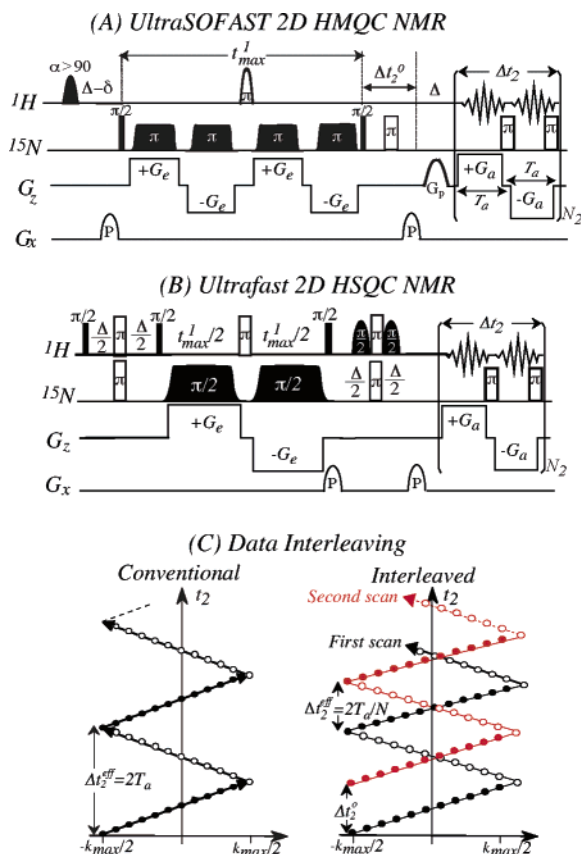
Figure 1. Ultrafast 2D NMR pulse sequences assayed toward the real-time characterization of protein dynamics. In all cases the frequency-chirped pulses applied for the sake of encoding the ^{15}N evolution were given WURST-like modulations and amplitudes suitable for executing $\pi/2$ or π nutations. Suppression of residual solvent signals was achieved by phase-cycling the first among the different ^{15}N pulses in concert with the receiver phase in a simple 2-step $(+x, -x)$ cycle; further clean ups of the undesired signals were introduced by short purging gradient pulses. (A) UltraSOFAST HMQC pulse sequence introduced in this study incorporating, in addition to a constant-time spatial encoding, amide-selective PC9 ^1H excitation pulses[33] applied at 8 ppm with a 4 ppm bandwidth and a flip angle $\alpha >$ 90°, optimized experimentally together with the subsequent REBURP[34] π-pulse for a given T_{scan} time. The delay Δ was set to 5.4 ms; the delay δ accounting for spin evolution during the PC9 pulse was adjusted in a 1D version of the experiment omitting all ^{15}N pulses to yield pure-phase spectra in the ^1H dimension. (B) Ultrafast HSQC pulse sequence based on an amplitude-modulation of the indirect domain,[35] incorporating Watergate[36] (aided by the non-encoding x-gradient) for the sake of solvent suppression. (C) Principle of the data interleaving procedure, incorporated in both of the assayed sequences (A,B) for eliminating imperfections. For the $N = 2$ case that is here demonstrated, an initial acquisition delay Δt_2^0 is set to 0 and $\Delta t_2/2$ in alternate scans (with an intermediate ^{15}N π-pulse for J-refocusing, panel A), and data collected under $+G_a$ (●) and $-G_a$ (○) gradients are combined in the interleaved fashion indicated by the scheme.

incremented-time versions owing to the ease with which constant-time procedures can simultaneously deal with the gradients and with an effective ^1H decoupling. Moreover, given that we sought an indirect-domain multiple-quantum dimension free from all ^1H effects, two such pairs of linearly swept ^{15}N inversion pulses were placed symmetrically with respect to the central ^1H refocusing pulse. In this way both the gradients as well as chemical shifts become effectively erased from the course of the ^1H evolution, and only ^{15}N effects are encoded.

As it was found that even with these provisions single-scan experiments failed to deliver the desired SNR for the targeted protein

concentration ranges, another provision was adopted to increase sensitivity: the multiscan acquisition of interleaved data transients. Acquiring spatially encoded scans in this manner (Figure 1C) is attractive because it alleviates the demands placed on the field gradients over the course of the acquisition. As a reminder,[38] data interleaving is an imaging-derived procedure that introduces $\Delta t_2^0(n) = \Delta t_2(n - 1)/N$ delays prior to acquisition of the $1 \le n \le N$ transient (with $\Delta t_2 = 2T_a$ the direct-domain dwell time, cf. Figure 1), and merges data obtained in such manner into a single set prior to Fourier transform along t_2. Whereas the direct-domain spectral width in single-scan acquisitions is given by $(2T_a)^{-1}$, this becomes $(2T_a/N)^{-1}$ after the data interleaving, thereby allowing one to increase the gradient oscillation time T_a by a factor N without compromising the direct-domain spectral width. This in turn allows one to reduce the acquisition gradient strength G_a by the same factor while preserving unaltered the indirect-domain spectral width, which is proportional to $k_{max} = \gamma_a T_a G_a$. Notice that in order to refocus the scalar coupling evolution occurring during the additional $\Delta t_2^0(n)$ delays a ^{15}N π-pulse was applied in their center; a two-scan $\pm 180°$ phase cycling was also generally incorporated on the initial ^{15}N excitation pulse of every interleaved set, leading to $N_{scans} = 2N$.

3. Results and Discussion

On the basis of the 2D ultraSOFAST HMQC sequence and processing strategy just described, a series of spectra on ^{15}N-labeled Ubiquitin were acquired for a variety of sample concentrations and acquisition times. Figure 2 shows representative spectra recorded in this manner on 500 and 800 MHz NMR spectrometers and compares them with a reference 500 MHz SOFAST 2D HMQC spectrum. As can be appreciated from this figure, the ultraSOFAST HMQC sequence clearly has the potential to discern a large number of resolved cross-peaks within ~1 s repetition rates, for proteins at ~2 to 3 mM concentrations. Comparisons between these 2D NMR data sets show clear resolution benefits upon going to higher magnetic fields; this is in part reflecting the relatively large line widths that all indirect-domain peaks exhibited as a result of having kept the encoding times relatively short (chosen in turn this way to prevent relaxation losses which might otherwise compromise sensitivity). On the other hand, the sensitivity enhancement resulting from the increase in field is only modest, in accordance to the B_o (as opposed to $B_o^{3/2}$) dependence expected for ultrafast experiments.[31]

To further explore the ultraSOFAST potential, a fast kinetic process, the hydrogen–deuterium exchange (H/D-exchange) in Ubiquitin, was monitored in real time. Knowing such H/D-exchange rates can give valuable insight into both the thermodynamics as well as the kinetics of local and global unfolding/folding of proteins in native conditions;[5,39,40] for the particular case of Ubiquitin, such rates of H/D exchange have been recently measured by a variety of 2D techniques including ultrafast HSQC[32] and Hadamard spectroscopy NMR.[41] For the present measurements an adaptation of the procedure described in ref 32 was used: 15 mg of ^{15}N-labeled lyophilized Ubiquitin were dissolved in 50 μL H_2O inside a Shigemi NMR tube, placed inside a properly tuned NMR system, and rapidly diluted by the addition of ~400 μL of D_2O. This injection was now

(34) Geen, H.; Freeman, R. *J. Magn. Reson.* **1991**, *93*, 93−141.
(35) Shrot, Y.; Shapira, B.; Frydman, L. *J. Magn. Reson.* **2004**, *171*, 163−170.
(36) Sklenar, V.; Piotto, M.; Leppik, R.; Saudek, V. *J. Magn. Reson. A* **1993**, *102*, 241−245.

(37) Pelupessy, P. *J. Am. Chem. Soc.* **2003**, *125*, 12345−12350.
(38) Matsui, S.; Sekihara, K.; Kohno, H. *J. Magn. Reson.* **1985**, *64*, 167−171.
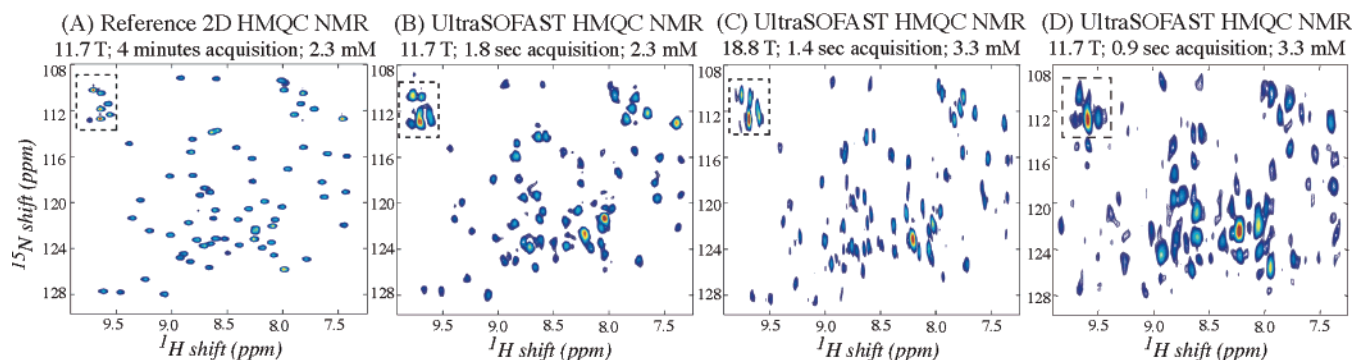(39) Arrington, C. B.; Robertson, A. D. *Biochemistry* **1997**, *36*, 8686−8691.
(40) Huyghues-Despointes, B.; Scholtz, J. L.; Pace, C. N. *Nat. Struct. Biol.* **1999**, *6*, 910−912.
(41) Bougault, C.; Feng, L.; Glushka, J.; Kupce, E.; Prestegard, J. H. *J. Biomol. NMR* **2004**, *28*, 385−390.

Figure 2. Comparison between 2D HMQC NMR spectra of ^{15}N-labeled Ubiquitin recorded under different conditions. The analyzed solution was prepared by dissolving the His-tagged powder (Asla Biotech) in a 90%/10% H$_2$O/D$_2$O phosphate buffer (pH = 7.5). As all remaining spectra in this manuscript, these data were collected at either 500 MHz on a Varian Inova equipped with a conventional triple-axis HCN probe head or at 800 MHz on a Bruker Avance equipped with a QXI probe. Dashed boxes contain folded peaks arising from amine groups. (A) Reference HMQC NMR spectrum defining the targeted peak positions and serving as a benchmark for our comparisons. This experiment relied on an optimized SOFAST protocol[15] and employed 128 t_1 increments with a four-scan phase cycle. (B) 500 MHz ultraSOFAST 2D HMQC NMR spectrum recorded using the pulse sequence in Figure 1A utilizing three interleaved scans, each of them with phase-cycling of the receiver and of the ^{15}N $\pi/2$ excitation pulse. Additional experimental parameters included G_e = 40 G/cm, rf sweep range = ± 16 kHz, t_1^{max} = 11.6 ms, N_2 = 15, T_a = 1.43 ms, G_a = 2.7 G/cm, a 2 μs physical acquisition dwell time, and ~6.8 kHz analog filtering of the data. Under these conditions, indirect- and direct-domain spectral widths of ~2500 and 1100 Hz were covered. Overall N_{scan} = 6 were collected at T_{scan} = 300 ms, leading to a 1.8 s total acquisition time. Data processing involved arranging the collected FIDs in the interleaved fashion shown in Figure 1C into two 715 × 60 $k/\nu_1,t_2$ data matrices (one corresponding to data collected with positive G_a and the other to negative G_a), zero-filling these sets to 2048 × 128, weighting along indirect and direct dimensions with a Gaussian function, 1D FT of both data sets along t_2, magnitude calculation of the spectra, and co-addition of both data sets for the sake of increasing SNR. (C) 800 MHz ultraSOFAST HMQC spectra recorded in a total time of 1.4 s using four interleaved scans (N_{scan} = 8 with the phase-cycling, T_{scan} = 175 ms). Other acquisition parameters involved G_e = 31.8 G/cm, rf sweep range = ± 35 kHz, t_1^{max} = 14 ms, N_2 = 16, T_a = 350 μs, G_a = 12.6 G/cm, a 2 μs physical acquisition dwell time, and ~125 kHz analog filtering of the data. (D) The same as in panel B but involving N_{scan} = 8 with T_{scan} = 112 ms resulting in a 0.9 s total acquisition time.

Scheme 1
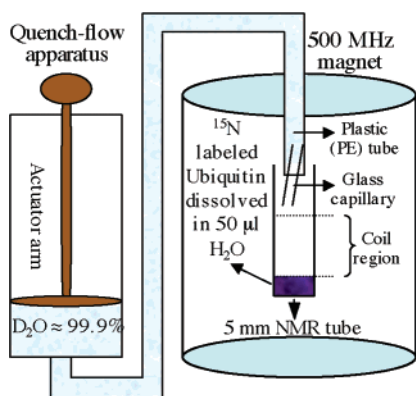
driven by triggering a KinTek RQF-3 quench-flow apparatus and channeled using a small custom-made nozzle placed inside the NMR tube in order to fill the sample coil region (Scheme 1). Although the solvent injection lasted itself a fraction of a second, ca. 1.5 s had to elapse in order to let the sample turbulence settle and enable the reliable acquisition of spatially encoded data. Even prior to this sudden D$_2$O injection the NMR spectrometer was already collecting ultraSOFAST HMQC spectra at a rate of one every 2.4 s. Further details on the parameters involved in this acquisition are given in the caption to Figure 3, which illustrates how the hydrogen−deuterium exchange manifests itself as a decay of the intensity of various NH resonances after the addition of D$_2$O. The data evidence the disappearance of various sites as a function of time, while probing lifetimes at faster rates and shorter dead-times (~0.4 Hz and 2 s) than had been approachable by our previous ultrafast dynamic studies for similar protein concentrations (~0.13 Hz and 30 s, respectively).[32] Some peak intensity profiles, chosen because of their relatively fast exchange kinetics, are displayed as a function of time after initiation of the experiments in Figure 4.

Given that a number of different ultrafast variants have been previously proposed and demonstrated for the recording of ^{1}H-^{15}N correlation spectra, it is pertinent to compare their general performance against the present ultraSOFAST experiments. Previous tests included HSQC versions carried out in sensitivity-enhanced and amplitude-modulated (am) modes.[35,37] The former achieved its encoding in combination with a double reverse-INEPT element retaining both orthogonal antiphase components,[42] yielding in principle a sensitivity advantage with respect to amHSQC. In practice, however, we did not witness these theoretical expectations; perhaps owing to the former's constant-time implementation leading to an enhanced transverse relaxation, or due to its additional INEPT step susceptible to increased relaxation or pulse-imperfection losses. In any case, in view of this behavior and given our more extensive experience with amHSQC NMR, we opted for comparing this ultrafast correlation protocol against the performance of the new ultraSOFAST HMQC sequence. With the monitoring of biomolecular dynamics as general objective, the target of such ultraSOFAST HMQC versus amHSQC comparison focused on measuring the sensitivity afforded by these different protein 2D NMR acquisition modes per unit time. Toward this end Figure 5A shows—using as a benchmark data obtained from comparable ultrafast amHSQC and ultrafast SOFAST HMQC acquisitions—how the normalized sum of intensities arising from identical, well-resolved peaks in each spectrum changes as a function of the duration of a single scan T_{scan}. The relative ratio between the intensities afforded by these two experiments is plotted in Figure 5B. These tests show that for relative long scan times (T_{scan} > 2 s) the performances of both experiments are comparable, suggesting that in this regime the potential T_2 losses of the multiple-quantum constant time ultraSOFAST HMQC evolution offset the gains that may arise from the enhanced spin-lattice

(42) Kay, L. E.; Keifer, P.; Saarinen, T. *J. Am. Chem. Soc.* **1992**, *114*, 10663−10665.
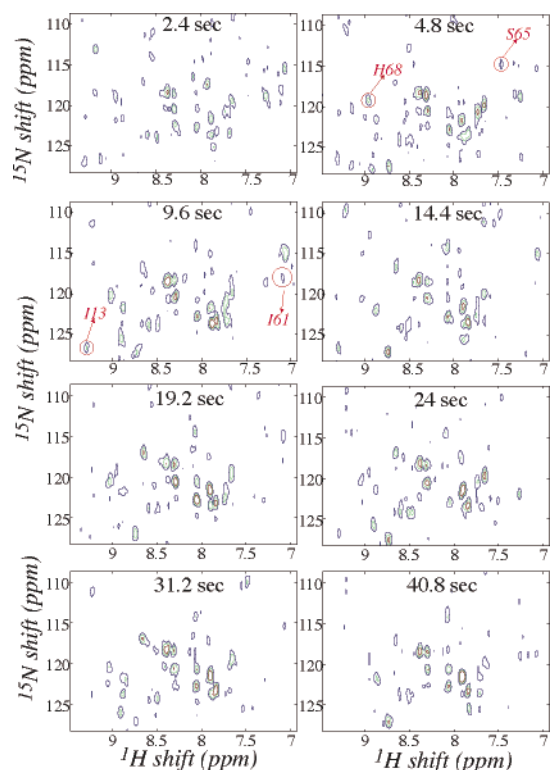
Figure 3. Representative series of real-time 2D ultraSOFAST HMQC NMR spectra recorded on a ~3 mM Ubiquitin solution, following the dissolution of an initially fully protonated lyophilized powder onto a D_2O-based buffer (final uncorrected pH = 8.9). The times indicated in each frame correspond to the approximate delay elapsed since the dissolution was suddenly triggered. Acquisition parameters were akin to those in Figure 2B (with $N_{scan} = 8$, $T_{scan} = 250$ ms) and so was the data processing. The repetition time between full recordings was ~2.4 s and data were monitored over a 20 min interval; only a subset of the collected and processed spectra is shown. The kinetics of the highlighted peaks are depicted by the corresponding graphs in Figure 4.

relaxation. For shorter T_{scan} times, however, on the order of 100−300 ms, the sensitivity of ultraSOFAST HMQC NMR exceeds that of amHSQC by up to a factor of 3. Within the context of fast acquisitions these curves imply that if the interscan delays are chosen at the maximum sensitivity of the SOFAST curve (~200 ms),[14,15] the ultraSOFAST HMQC will give sensitivity gains of ca. 2 over its amHSQC counterpart for the same total acquisition times, and that if even faster repetition rates are desired, the ultraSOFAST gain could lead to factors approaching 3 for identical experimental times.

Less satisfactory but also important to include in an SNR comparison, is the issue of water suppression. Good water suppression is of course a crucial procedure that is challenged in rapid-mixing ultrafast NMR by two nonconventional issues. One of these relates to the fact that sudden injections of the kind illustrated in Scheme 1 will usually take place on unshimmed samples susceptible to initial turbulence and foaming, factors which, when combined, lead to less-than-optimal peak line widths. Another concern arises from the fact that in ultrafast NMR, the spectral width associated to the physical data sampling is usually kept larger than normal to allow for the simultaneous digitization of the two spectral axes; an undesired folding-over of residuals and/or forbidden echoes from the water signal is therefore facilitated. We found, for instance, that water-flip back schemes of the kind usually employed in standard
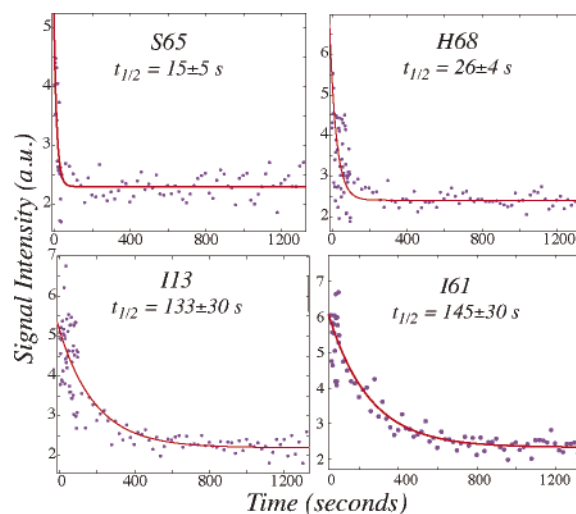
Figure 4. H/D exchange plots extracted from the data in Figure 3 for four residues exhibiting fast kinetic processes. Experimental points reflect peak heights in the ultraSOFAST HMQC 2D spectra; the $t_{1/2}$ exchange lifetimes given in the figure were obtained by fitting the data points to the equation $I(\tau) = I_o \exp(-\tau/t_{1/2}) + I_\infty$. The points chosen over the course of the first 50 measurements (time $\tau \leq 120$ s) arise from full separate 2D acquisitions, each of these 2.4 s long. Thereafter, for the sake of reducing scattering and in view of the slowing down of the dynamics, ten consecutive spectra (50 through 60, 60 through 70, etc.) were co-added and the exchange time was assigned to the center time of this average. We ascribe the shorter lifetimes arising from these fits vis-à-vis their counterparts reported in ref 32, to the higher pH's (8.9 vs 6.5) in which measurements were now performed.

HSQC experiments[43] are usually insufficient for acquiring dynamic ultrafast amHSQC spectra, unless extensive phase cycling of the encoding pulses is used. UltraSOFAST HMQC, which uses selective pulses not to store back but rather to minimize the overall water excitation, is also handicapped in the quality of its water suppression. Indeed we found that the reliance on such selective spectral manipulations did not yield, following a basic $\pm x$ two-scan phase cycling, as complete a water suppression as that observed in ultrafast experiments incorporating Watergate-type schemes—particularly when the latter relied on gradient dephasing along a transverse, non-encoding axis. The partial excitation occurring in ultraSOFAST HMQC NMR of the H_2O background was particularly noticeable in the rapid-mixing 500 MHz tests; these interferences were weaker at 800 MHz, where the separation between the water resonance and the amide region exceeds 3 kHz. On the other hand, in experiments like those in Figure 3 relying on dilution by a mostly deuterated solvent, these water suppression issues were not severe. The SOFAST procedure had the added advantage of keeping the H_2O magnetization always in thermal equilibrium; this was an aid for observing amides at neutral or basic pH (e.g., pH 8.9 in Figure 3) whose protons are prone to undergo rapid exchange with water molecules and thus lead to SNR losses if using saturation/dephasing of the H_2O resonance. Still, we ascribe the longer signal averaging times that were needed in the rapid-mixing, mostly deuterated solvent experiments (Figure 3) over those carried out in equilibrated protonated solutions (Figure 2) to the need to overcome noise problems arising from incomplete solvent suppression, rather than to inherent limitations in the available signal.

(43) Kay, L. E.; Xu, G. Y.; Yamazaki, T. *J. Magn. Reson. A* **1994**, *109*, 129−133.
(44) Schanda, P.; Brutscher, B. *J. Magn. Reson.* **2006**, *178*, 334−339.
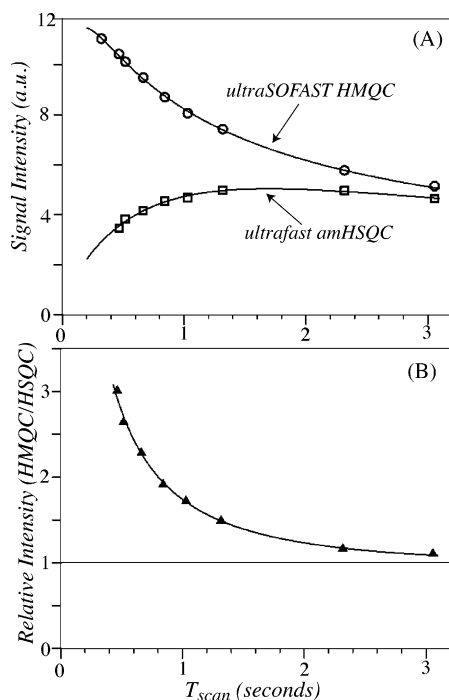
Figure 5. Experimental comparison between spatially encoded ultraSO-FAST HMQC and amHSQC NMR experiments, as given by the signal per unit time of 2D ^{15}N-^{1}H correlation spectra recorded with each sequence (amHSQC, open triangles; ultraSOFAST, HMQC open circles). The acquisition parameters were set akin to those introduced in Figure 2; the duration of each frequency-chirped pulse was set to 11.6 ms for the amHSQC and 2.9 ms for the ultraSOFAST HMQC experiments, resulting in a t_1^{max} that is twice as long for the former than for the latter and thereby yielding the same effective degree of encoding for both experiments. The data points whose intensity are plotted on the top graph as a function of T_{scan} were obtained by summing the intensities of 17 identical, well-resolved cross-peaks in both spectra. Each spectrum was recorded in the same total time (set to 74 s to increase the precision of the obtained data) and scaled to the same noise level according to the number of scans. The intensity ratio between both data sets is indicated by the filled triangles of the lower plot, with a line at a ratio of 1 added as visual aid. Both curves in panel A should converge to zero as $T_{scan} \rightarrow 0$; in the present case, T_{scan} was kept ≥ 200 ms (which corresponded to essentially the maximum of the ultra-SOFAST HMQC curve) as at shorter recycle delays the gradient amplifier employed would exceed its duty-cycle capabilities.

4. Conclusion

A new 2D NMR pulse scheme for the acquisition of ^{1}H-^{15}N correlation spectra at $\sim$2 mM protein concentrations and at repetition rates approaching 1 Hz was presented, combining the benefits of SOFAST HMQC and of spatial encoding. Although previously presented spatially encoded techniques had been able to yield a 2D protein HSQC NMR spectra in a single scan, practical sensitivity considerations makes this possible only at relatively high concentrations (ca. 3 mM for state-of-the-art hardware). Moreover, monitoring protein dynamics by executing such multiple HSQC acquisitions at high repetition rates would still be challenged by the usual requirements of spin relaxation. The proposed combination of SOFAST and ultrafast techniques is definitely a valuable step toward alleviating this situation, enabling the repetition of 2D NMR measurements at the highest possible frame rate. In fact SOFAST HMQC NMR has already been shown compatible with another fast acquisition method, Hadamard-encoding, a combination which decreases the number of necessary scans significantly and also allows one to record 2D ^{1}H-^{15}N correlations within second-long timescales.[44] Unlike Hadamard spectroscopy, however, the proposed spatially encoded ultraSOFAST HMQC experiment results in full 2D spectral correlations rather than in a series of 1D projections, yielding an unbiased range of spectral changes along both dimensions. We believe that this may be an aid to study processes where peak positions might be changing owing to the dynamics, as would be the case upon following protein folding. We trust that, with further increases in sensitivity brought about by advances in magnet and probe technology and with additional pulse-sequence developments including better approaches to solvent suppression, the proposed experiment will eventually become a useful route to study fast biomolecular kinetics at a site-resolved level and within subsecond timescales.

JA066915G